EMPIRICAL IMPACT EQUATIONS AND MARGINAL PERFORATION.

L. Berthoud and J.C. Mandeville

CERT-ONERA/DERTS
2 Av. E. Belin, 31400 Toulouse, France
Fax: (33) 61 55 71 69

ABSTRACT

The arrival of LDEF and Mir 'Aragatz' samples exposed to the Low Earth Orbit (LEO) particle environment has provided the stimulation for the present reexamination of empirically-developed impact equations. In order to interpret the flux observed by the experiments, impact equations are needed to convert observed crater dimensions to impacting particle dimensions. This paper presents the results of recent simulation experiments, whose objective was the selection of suitable equations for the space-exposed samples. The experiments used mm- and µm-sized Fe projectiles impacting Al samples similar to those exposed in space at velocities from 1 to 14 km/s.

The results allow an assessment of both empirical equations and alternative parameters proposed to characterise impacts (such as f/D: (target thickness) / (crater diameter)). The influence of equation choice on particle flux predictions is shown. This difference may account for the differences in flux found by different investigators. Our conclusions also shed light on the quantitative description of marginal perforation. This subject, also tackled by McDonnell (Ref. 1), Hörz (Ref. 2) and Humes (Ref. 3), holds the key to a global understanding of the process of impact damage. The improvements to the description of material behaviour upon hypervelocity impact presented here will help flux interpretation from space-exposed samples and spacecraft shield design.

NOMENCLATURE

c_t	: velocity of sound in target (km/s)
D	: Crater diameter (cm)
d	: Particle diameter (cm)
ε	: foil ductility (0.4 for Al foils)
f	: foil/target thickness (cm)
H	: Brinell hardness (90 for 6061-T6 Al)
P	: Penetration depth (cm)
ρ_p	: density of projectile (g/cm^3)
ρ_t	: density of target (or 'foil') (g/cm^3)
σ_{Al}	: tensile strength of Aluminium (80 MPa for 6061 Al)
σ_t	: tensile strength of target (MPa)
V	: velocity of impact (km/s)

1. INTRODUCTION

To design a spacecraft for a mission into the micrometeoroid and debris environment, it is necessary to characterise the response of structural materials to hypervelocity impact. Empirically developed equations provide simplified descriptions of the damage caused by impact. This damage can be broadly divided into three classes: *craters*, where the particle is stopped by the target, *perforations*, where the particle passes through the target completely, and *marginal perforations*, where the particle barely passes through the target.

No reasonable simplified analytical description of plate penetration exists. The impact process inherently involves complex large multi-dimensional deformations and demands detailed descriptions of plastic flow and fracture with accompanying accurate material property determinations at appropriate strain rates. Powerful hydrodynamic codes are being developed to solve the partial differential equations governing the process. But as long as these hydrocodes remain limited in application and costly to run, empirical fits to experimental data can provide a simple and rapid alternative.

2. EMPIRICAL EQUATIONS

Numerous empirical and semi-empirical relationships have been developed to convert crater/perforation morphology to particle mass/diameter, equivalent crater size in aluminium or equivalent penetration thickness. All these methods depend on assumptions about projectile densities, velocities and interaction with the target. The equations are developed using regression methods to approximate particle impact simulations carried out in the laboratory. McDonnell and Sullivan, (Ref. 4) give a description of the typical development of an empirical equation.

There are three different sets of equations which cover the three different thickness regimes. Our goal was to find appropriate D/d ratios for each regime. In this paper the equations are converted to the same format for comparison purposes.

2.1 Semi-infinite P/d Equations

These are applicable to the semi-infinite or 'thick' target regime where cratering occurs. They were developed principally for shielding considerations where the crater

depth P was considered the most important parameter. In order to find out D/d, the ratio P/D must be assumed:

$$\frac{P}{d} = \frac{P}{D}\cdot\frac{D}{d} \qquad (1)$$

2.1.1. Cour-Palais and Christiansen (Ref. 5 based on 6)

Al targets, particles 50 μm<d<1.3 cm, V< 12 km/s

$$\frac{P}{d} = \frac{5.24\ d^{0.056}}{H^{0.25}} \left(\frac{\rho_p}{\rho_t}\right)^{0.5} \left(\frac{V}{c_t}\right)^{0.667} \qquad (2)$$

2.1.2. Pailer and Grün (Ref. 7)

Iron and polystyrene μm-sized particles impacting various films and other collected data, 1 ≤ V ≤ 20 km/s.

$$\frac{P}{d} = \left(\frac{0.772}{\varepsilon^{0.06}\ \rho_t^{0.5}}\right) d^{0.21}\ \rho_p^{0.73}\ (V\cos\theta)^{0.88} \qquad (3)$$

2.1.3. NASA (Ref. 8):

Metal targets,

$$\frac{P}{d} = K_\infty\, d^{0.056}\, \rho_p^{0.519}\, V^{0.667} \qquad (4)$$

where K_∞ is a target material constant (0.42 for Al and 0.25 for stainless steel).

2.1.4. Kineke (Ref. 9):

Metallic targets, mm- and cm-sized projectiles, 2-5 km/s. NB: V is in cm/s here.

$$\frac{D}{d} = K_1\, \rho_p^{0.333}\, V^{0.667} \qquad (5)$$

$$\frac{P}{d} = K_2\, \rho_p^{0.333}\, V^{0.667} \qquad (6)$$

K1 and K2 depend on target and projectile materials (K1 is 3.8×10^{-4} and K2 is 5.8×10^{-4} for steel onto Al)

2.2. Marginal Thickness f/d Equations

Marginal perforation equations are a special case of P/d equations. They apply to 'marginal thickness' plates ie: the plate thickness at which a crater becomes a perforation, where the projectile barely perforates the target. Instead of crater depth P, the critical parameter is the target thickness at marginal perforation: 'f'. These equations were developed principally for calculating the detection limit of thin metal foils.

2.2.1. McDonnell and Sullivan (Ref. 4),

Fe μm-sized particles impacting various films, 2 ≤ V ≤ 20 km/s.

$$\frac{f}{d} = 1.023\, d^{0.056} \left(\frac{\rho_p}{\rho_t}\right)^{0.476} \left(\frac{\sigma_{Al}}{\sigma_t}\right)^{0.134} V^{0.664} \qquad (7)$$

2.2.2. Nauman (Ref. 10),

10-100 μm-sized borosilicates impacting metallic targets, 4 ≤ V ≤ 13 km/s.

$$\frac{f}{d} = d^{0.056}\ \rho_p^{0.52}\ V^{0.875} \qquad (8)$$

2.2.3. Cour-Palais (Ref. 11),

$$\frac{f}{d} = 0.635\ \rho_p^{0.52}\ d^{0.056}\ V^{0.67} \qquad (9)$$

2.2.4. Fish and Summers (Ref. 12),

Aluminium mm-sized particles impacting metallic targets, 1 ≤ V ≤ 5 km/s.

$$\frac{f}{d} = 0.43\ \rho_p^{0.52}\ d^{0.056}\ V^{0.875} \qquad (10)$$

2.2.5. Pailer and Grün (Ref. 7)

Iron and polystyrene μm-sized particles impacting various films and other collected data, 1 ≤ V ≤ 20 km/s.

$$\frac{f}{d} = \left(\frac{0.772}{\varepsilon^{0.06}\ \rho_t^{0.5}}\right) d^{0.21}\ \rho_p^{0.73}\ (V\cos\theta)^{0.88} \qquad (11)$$

2.2.6. Humes (Ref. 3)

Deduced from Explorer and Pegasus data and from equation (4), 4<V<20. (K3 is 0.72 for Al targets).

$$\frac{f}{d} = K3\ \rho_p^{0.166}\ d^{0.056}\ V^{0.667} \qquad (12)$$

2.2.7. CTH hydrocode (Ref. 13)

Aluminium impacting aluminium, $4 \leq V \leq 15$ km/s.

$$f = 0.81\ d^{0.9375}\ V^{0.625} \qquad (13)$$

2.3 Finite D/d Equations

These equations apply to finite or 'thin' targets where perforation occurs.

2.3.1. Sawle (Ref. 14),

Thin foils;
0.88<D/d<3.7; 0.083<f/d<0.33; 11<V<17 km/s.

$$\frac{D}{d} = 1 + 3.2 \left(\frac{\rho_p\ V}{\rho_t\ c_t}\right)^{0.2} \left(\frac{f}{d}\right)^{0.667} \qquad (14)$$

2.3.2. Maiden, Gehring and McMillan (Ref. 15),

Thin Al foils;
1.0<D/d<3.5; 0.04<f/d<0.5; 1<V<8 km/s.

$$\frac{D}{d} = 0.45 \left(\frac{f}{d}\right)^{0.667} V + 0.9 \qquad (15)$$

Revised version (Ref. 16),

$$\frac{D}{d} = 2.4\ \frac{V}{c_t} \left(\frac{f}{d}\right)^{0.667} + 0.9 \qquad (16)$$

2.3.3. Schonberg, Taylor and Horn (Ref. 17),

Thin Aluminium foils;
1.5<D/d<3; 0.2<f/d<0.33; 5<V<8 km/s.

$$\frac{D}{d} = 1.12 + 2.794 \left(\frac{V}{c_t}\right)^{0.962} \left(\frac{f}{d}\right)^{0.895} \qquad (17)$$

3. SIMULATION EXPERIMENTS

The following experiments were carried out to enable the selection of empirical equations for the space-exposed samples. Testing was done at both ends of the possible particle size range: 0.4-4 μm (using an electrostatic accelerator) and 0.5 cm (using a light gas gun).

3.1. Choosing a semi-infinite P/d equation and verifying size-scaling effect.

Electrostatic accelerator (MPI, Heidelberg)
Projectiles: Known diameter Fe spheres
Targets: 50 μm Al (99% pure) foils
Velocities: 1, 3, 5.5, 8, 10, 12, 14 km/s

Light gas gun (CEG, Gramat)
Projectiles: 5mm steel sphere
Target: 20x15 cm Al (6061 T6) block
Velocities: 4, 5, 6, 7, 8 km/s

3.2. Finding marginal perforation thickness and choosing an appropriate f/d equation.

Electrostatic accelerator (MPI, Heidelberg)
Projectiles: Known diameter Fe spheres
Targets: 0.8, 2, 5 μm Al (99%) foil
Velocity: 5.5 km/s

3.3. Choosing a finite D/d equation.

Electrostatic accelerator (MPI, Heidelberg)
Projectiles: Known diameter Fe spheres
Targets: 0.8 μm Al (99% pure) foils
Velocity: 5.5 km/s

3.4. Measurements

For the μm impacts, interior crater diameters were measured at the sample surface using the microscale on the SEM (following the guidelines indicated in See (Ref. 18)). Crater depths were measured using stereoscopic images. Errors including measurement errors and the uncertainty of particle diameter and velocity determination for the particle accelerator are estimated at ± 20%.

4. RESULTS

4.1. Impacts in Semi-infinite Targets

Figure 1 shows a comparison of experimental values of D/d with calculated values, using different empirical equations. The experimental value of P/D was used to convert from P/d for the calculated values (see figure 3). The graph shows that the experimental results approximate those predicted by the NASA equation.

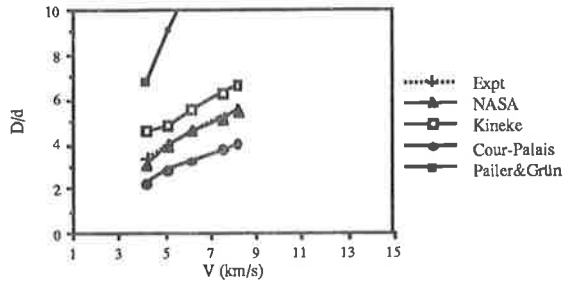

Figure 1: Calculated and experimental simulation D/d values against velocity V for steel projectiles impacting aluminium (mm-sized impacts).

Figure 2 shows the equivalent graph for the μm-sized impacts. The experimental values of D/d appear to coincide best with the Cour-Palais equation, although the Pailer and Grün values are also similar. The higher experimental values for low velocity values may be due to the difficulty of estimating the real depth of a crater when the projectile still remains partially inside it. The experimental values appear to follow the $V^{0.667}$ rule, consistent with energy considerations.

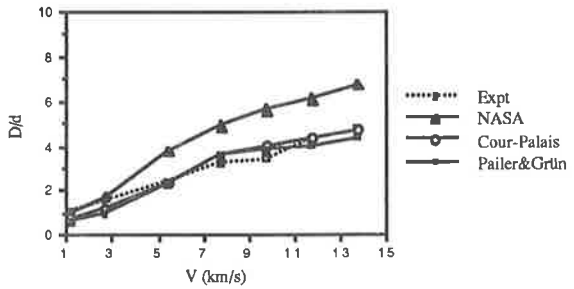

Figure 2: Calculated and experimental simulation values of D/d against velocity for iron particles impacting pure Al foils (μm-sized impacts).

Figure 3 shows the measured crater depth to diameter ratio P/D for the light gas gun and accelerator experiments. There is a significant size-scaling effect: at hypervelocities the μm impacts have an average P/D of 0.6 whilst the mm impacts average 0.88. This effect could be due to the difference in target material properties, which are taken into account in Pailer and Grün but not in NASA (see Ref. 19 for details).

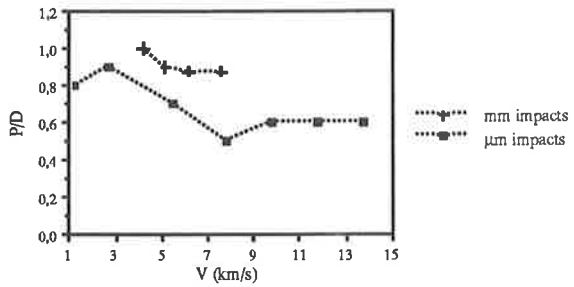

Figure 3: Comparison of experimental P/D measurements against velocity for mm impacts (light gas gun) and μm impacts (electrostatic accelerator).

The size scaling effect for D/d is shown in figure 4. It seems that the Cour-Palais equation fits at the micron end and the NASA fits at the mm end, but neither increase rapidly enough with projectile diameter. The Pailer and Grün equation increases too rapidly with projectile diameter.

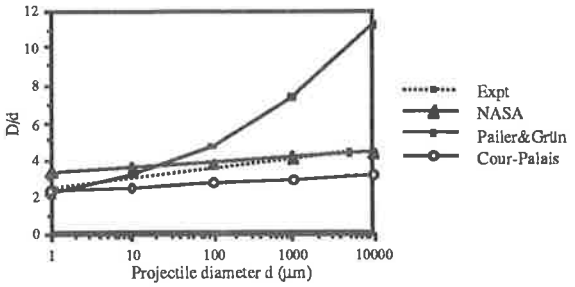

Figure 4: Calculated and experimental simulation values for D/d against d for Fe impacts onto Al targets at 5.5 km/s

4.2. Impacts on Marginal Thickness Targets

A comparison of calculated and experimental values for marginal thickness (Figure 5) shows that the McDonnell and Sullivan, Fish and Summers and Cour-Palais equations all give estimates fairly similar to the experimental values for μm impacts. The differences in the equations may be explained by different interpretations of the term 'marginal perforation'. These vary from 'light tight' to 'pressure tight' to 'breakaway of spallation'. The differences can be clearly seen from Hörz's experimental results for impacts on the mm scale. Experiments by the authors show that the development of a perforation on the μm scale is similar. The scaling effect for mm-impacts will be verified in the next series of tests using the CEG Gramat light gas gun.

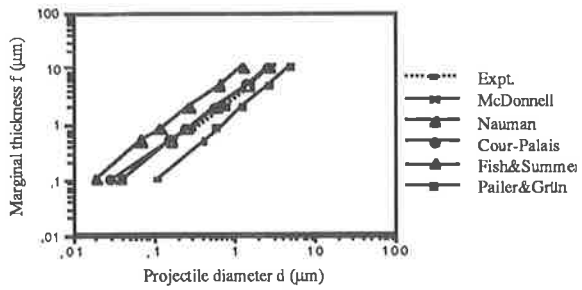

Figure 5: Calculated and experimental simulation values for Fe impacting Al foils at 5.5 km/s (μm impacts).

Marginal f/D is a measure analogous to P/D and as such we assume it is constant for 4<V<20 km/s but remains dependent on target and particle densities. This is borne out by observations: for the above experiments marginal f/D=1.0, whereas for space-exposed targets where the particle density is thought to be lower, f/D for marginal perforations was found by the authors to be 0.65-0.75. McDonnell (Ref. 20) also found f/D=0.68 for the LDEF MAP samples.

4.3. Impacts on Finite Targets

It is important to note the experimental conditions (and hence limits of validity) of the finite target equations. These are given in a convenient form by Schonberg (Ref. 17). Figure 6 which compares empirical equation and experimental values for D/d for normalised foil thickness f/d. NB: f is in this case foil thickness and not marginal thickness as for the previous set of equations.

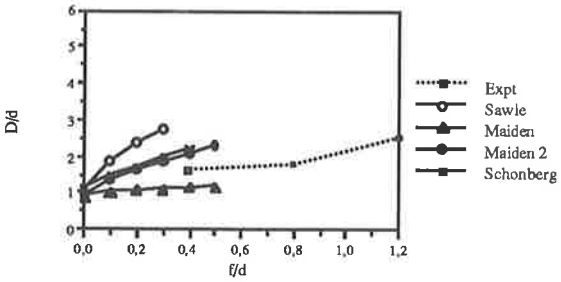

Figure 6: Calculated and expt. simulation values of D/d against f/d for Fe impacts on Al foils at 5.5 km/s.

4.4. Conversion from crater to particle dimensions

From the above results we have selected the following equations:

Semi-infinite targets:	Cour-Palais for μm impacts
	NASA for mm-sized impacts,
Marginal thickness:	McDonnell and Sullivan,
Finite Thickness:	Maiden (version 2).

For all interpretations of craters in space-exposed samples, the impacting projectile velocity and density must be assumed. Here, for the purposes of conversion, the following assumptions are made:
V = 15 km/s; ρ_p = 3.5 g/cm^3; P/D = 0.62

Figure 7 shows the conversion of the raw crater flux data from a semi-infinite target on the LDEF trailing edge (expt. A0138-1). We can see that the NASA equation predicts a lower flux than Cour-Palais, and that Pailer and Grün gives a higher flux for small particle diameters and a lower flux for larger diameters. This could explain why the flux calculated for Solar Max (Ref. 21) using this equation is higher than that found for LDEF.

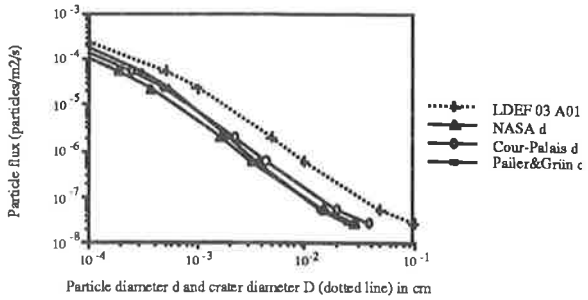

Figure 7: Particle flux against LDEF observed crater diameter (dotted line) with conversions to particle diameter, using different semi-infinite equations.

The particle diameters necessary to cause marginal perforation in the in space-exposed targets (using the McDonnell and Sullivan equation and the above particle assumptions) are given below. These values provide the limit for the application of the semi-infinite equations. Then there is a gap from f/d=4 to f/d=0.5 not covered by equations. From f/d<0.5 the finite target equations become valid:

f = 0.8 μm, (marg) d = 0.2 μm, (finite) d > 1.6 μm
f = 2 μm, (marg) d = 0.5 μm, (finite) d > 4 μm
f = 5 μm, (marg) d = 1.2 μm, (finite) d > 10 μm
f = 50 μm, (marg) d = 10.5 μm, (finite) d > 100 μm.

For these, there is no elegant way to extract the particle diameter d. A short bisection program is used by the authors to give a numerical approximation of d.

A rather unsatisfactory grey area between marginal and finite equations remains. This is illustrated in figure 8 with the conversion of crater (created by smaller impactors) and perforation (created by larger impactors) diameters measured on a 5 μm foil exposed on the Mir station (Ref. 22) to particle diameters. The figure shows that the crossover in validity between the thick (for craters) and thin (for perforations) equations occurs at approx. d = 9 μm. Great care must be taken in applying empirical equations to flux measurements for foil thicknesses which fall within the marginal perforation regime.

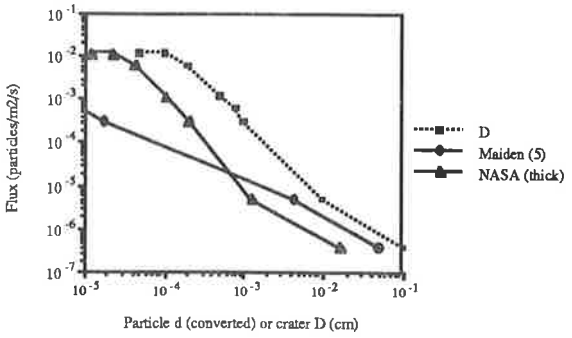

Figure 8: Particle flux against observed crater diameters (dotted) on Mir 5μm foil with semi-infinite (NASA) and finite (Maiden) conversions to particle diameter.

5. CONCLUSIONS

In this paper, simulation experiments were used to select suitable impact equations for the conversion of crater geometry to impacting particle diameter for space-exposed samples. A significant size-scaling effect was observed for the semi-infinite target experiments. This suggests that the particle diameter coefficient needs adjusting. Further tests are planned to investigate size-scaling for marginal thickness and finite targets.

The influence of the choice of equations on the interpretation of flux is demonstrated. Consideration of target thickness, material characterisitics and particle size are all important factors in this choice. The difference in flux values given by different models may explain apparent differences between Solar-Max and LDEF flux and between different LDEF investigators.

6. REFERENCES

1. McDonnell J. (1970) "Factors affecting the choice of foils for penetration experiments in space" in '*Space Research X*', proc. of 12th Cospar meeting, Prague, 1969. Publ. North Holland Pub. Co.

2. Hörz F., Cintala M., Bernhard R.P. and See T.H. (1992) "Dimensionally scaled penetration experiments: aluminium targets and glass projectiles 50 μm to 3.2 mm in diameter", submitted to '*Int. Journal of Impact Eng.*'

3. Humes D.H. (1991) "Large craters on the meteoroid and space debris impact experiment" in part 1 of '*LDEF-69 Months in Space, First Post-Retrieval Symposium*' NASA Conf. Publ. 3134.

4. McDonnell J.A.M. and Sullivan K. (1992) "Hypervelocity impacts on space detectors: decoding the projectile parameters" in '*Hypervelocity Impacts in Space*', ed. McDonnell J.A.M., publ. Univ. of Kent at Canterbury, GB.

5. Hörz F. et al. (1991) "Preliminary analysis of LDEF expt. A0187-1 'Chemistry of micrometeroid expt.'in part 1 of '*LDEF-69 Months in Space, First Post-Retrieval Symposium*' NASA Conf. Publ. 3134.

6. Cour-Palais B.G. (1987) "Hypervelocity impacts in metals, glass and composites", *Int. J. Impact Eng.* 5, pp681-692.

7. Pailer N. and Grün E. (1980) "The penetration limit of thin films", *Planet. Space Sci.* Vol. 28, pp. 321-331. Pergamon Press Ltd. GB.

8. *NASA SP-8042* (1970) "Meteoroid damage assessment".

9. Rudolph V. (1967) Doktorarbeit, MPI Heidelberg.

10. Nauman R. (1966) *NASA TND 3717.*

11. Cour-Palais B.G. (1979) "The comet Halley micrometeoroid hazard workshop", *ESA SP-153*, p.85.

12. Fish A.H. and Summers J.L. (1965) "The effect of material properties on threshold perforation", *Proc. 7th Hypervelocity Impact Symp.*

13. LDEF Meteoroid and Debris Special Investigation Group (1992) "*Meteoroid and debris interim report*".

14. Sawle D. (1960) "Hypervelocity impact in thin sheets and semi-infinite targets at 15 km/s", LRL, UCB, *AIAA Hypervelocity Impact Conf.* Cincinatti.

15. Maiden C.J., Gehring J.W. and McMillan A.R. (1963) "Investigation of fundamental mechanism of damage to thin targets by hypervelocity projectiles", *NASA-TR 63-225.*

16. Maiden C.J. and McMillan A.R. (1964) "An investigation of the protection afforded a spacecraft by a thin shield", *AIAA J.* Vol. 2, No. 11, pp1992-1998.

17. Schonberg W.P., Taylor R.A. and Horn J.R. (1988) "An analysis of penetration and ricochet phenomena in oblique hypervelocity impact", *NASA TM-100319.*

18. See T.H., Allbrooks M.K., Atkinson D.R. et al. (1991) "Meteoroid and debris special investigation group data acquisition procedures", part 1 of '*LDEF-69 Months in Space, First Post-Retrieval Symposium*' NASA Conf. Publ. 3134.

19. Gehring J. (1970) "Engineering considerations in hypervelocity impact", p463 of '*High-Velocity Impact Phenomena*' ed. R. Kinslow, publ. Academic Press.

20. McDonnell J.A.M. et al. (1992) "Impact cratering from LDEF's 5.75 yr exposure", *Proc. Lunar. Planet. Sci.* Vol. 22, pp.185-193.

21. Warren J., Zook H.et al. (1989) "The detection and observation of meteoroid and space debris impact features on the Solar Max satellite", *proc. 19th Lunar and Planetary conf.* pp.641-657.

22. Mandeville J.C. and Berthoud L. (1993) "Orbital debris and meteoroids: results from retrieved space experiments", *this conference.*

7. ACKNOWLEDGEMENTS

Thanks to Professor Eberhard Grün and his department, in particular Herr Gerhard Schäfer, for their help during testing at the Max Planck Institut für Kernphysik, Heidelberg. Also to Messieurs Pierre Chartagnac and Christian Loupias for their cooperation during testing at the Centre d'Etudes de Gramat. This work was supported by a grant for research at CERT-ENSAE, Toulouse, from the European Commission within the 'Science' programme.